www.amlett.com, www.vbripress.com/aml, DOI: 10.5185/amlett.2015.5901 Published online by the VBRI Press in 2015

# Synthesis of nickel nanoparticles: Microscopic investigation, an efficient catalyst and effective antibacterial activity

**Ratiram Gomaji Chaudhary[1*], Jay A. Tanna[1,4], Nilesh V. Gandhare[2], Alok R. Rai[3], Harjeet D. Juneja[4]**

[1]*P.G. Department of Chemistry, Seth Kesarimal Porwal College, Kamptee, RTM Nagpur University, Kamptee 441001, India*
[2]*Department of Chemistry, Nabira Mahavidyalaya, Katol, RTM Nagpur University, Katol 441302, India*
[3]*P.G. Department of Microbiology, Seth Kesarimal Porwal College, Kamptee, RTM Nagpur University, Kamptee, India*
[4]*Post Graduate Teaching Department of Chemistry, RTM Nagpur University, Nagpur 440033, India*

[*]Corresponding author. Tel: (+91) 9860032754; E-mail: chaudhary_rati@yahoo.com; ratswat81@yahoo.com

**Received: 03 March 2015, Revised: 11 July 2015 and Accepted: 15 July 2015**

## ABSTRACT

Nickel nanoparticles (Ni NPs) with a crystalline size of around 30 nm have been synthesized successfully via the chemical reduction method. Ni NPs were obtained through a nickel salt with hydrazine hydrate at 80 °C temperature by using ethylenediamine as protective agent. The synthesized nanoparticles were characterized by using FTIR spectroscopy, powder X-ray diffraction pattern, ultraviolet-visible spectroscopy, energy dispersive X-ray spectroscopy (EDS), thermogravimetry (TG/DTG), scanning electron microscopy (SEM) and transmission electron microscopy (TEM). The size and morphology behavior of NPs were studied by PXRD, SEM and TEM techniques. Furthermore, its applications studies were carried out as catalyst for Knoevenagel condensation reaction of aromatic aldehydes and malononitrile under solvent free conditions. The efficacy of NPs catalyst was exhibited an excellent recyclability and reusability up to four times without any additional treatment. The silent feature of nickel nanoparticles were found as efficient, cleaner reactions profiles and simple workup. Moreover, its comparative antibacterial activities were performed by using common solvents and sonication under standard method. The antibacterial activities were tested against human bacterial pathogen such as Staphylococcus aureus, Escherichia coli, Klebsiella sp, Enterococcus faecalis and Pseudomonas aeruginosa using well diffusion method. Nonetheless, the antibacterial activities of Ni nanoparticles (20 to 60 ug) were compared with four well known antibiotics i.e. Amikacin (30 mcg), Ciprofloxacin (5 mcg), Gentamicin (5 mcg) and Norfloxacin (10 mcg). The highest antimicrobial activity of Nickel nanoparticles were found against Pseudomonas aeruginosa, Staphylococcus aureus (21 mm) and Klebsiella sp. (20 mm). However, the results reveal an efficient antimicrobial activity against pathogenic bacteria under sonication than common solvent technique. 

**Keywords:** Nickel NPs; TEM; efficient catalyst; knoevenagel condensation; antibacterial activity.

## Introduction

The synthesis of nanoparticles is of current interesting endeavor for researcher due to their tremendous applications in different areas because of their novel properties and small dimensions **[1]**. Nowadays, the synthesis of metal nanoparticles has received considerable attention because of their extremely applications such as electrical, magnetic, thermal, sensor devices, biological and chemical properties, especially catalytic properties which did not achieve from those of the bulk materials **[2-4]**. Therefore, various researchers around the different continents are trying to prepare metal materials at the nano scales. Particularly, for the synthesis of transition metal nickel nanoparticles (Ni NPs) have gained tremendous importance in the last two decades as they posses good catalyst for organic compounds synthesis, biological activities, an efficient and reusability of catalyst **[5, 6]**. Also, the recent literature survey reveals that the nano nickel used as heterogeneous catalyst and received noteworthy attention because of its inexpensive, non-toxic, low corrosion, waste minimization, easy transport and disposal of the catalyst **[7]**. However, the better efficiency of heterogeneous catalysis in organic synthesis can be improved by employing nanosized catalysts because of their extremely small size and large surface to volume ratio. During the recent years most of the work done on Ni NPs as catalysts which offer great opportunities for wide range of applications in organic synthesis and chemical manufacturing processes including the chemo selective oxidative coupling of thiols **[8]**, synthesis of tetraketones and *bis*-coumarins **[9]**, reduction of p-nitrophenol **[10]**, polyhydroquinoline derivatives **[11]**, and bis (indolyl) methane synthesis **[12]** which supports for hydrogen adsorption **[13]**. Generally, Ni NPs are unstable and the exploration of appropriate support for stabilizing catalytic

nanoparticles is a key factor in their successful and wide applications in heterogeneous catalysis **[14]**. Thus, the remarkable catalytic activity, facile synthesis, ecofriendliness and recoverability of the Ni NPs encouraged us to utilize this as catalyst for the Knoevenagel condensation of aromatic benzaldehyde and malononitrile.

On the other hand, the Knoevenagel condensation is one of the most useful and widely employed methods for organic synthesis which have numerous applications in the synthesis of fine chemicals, hetero Diels-Alder reactions and carbocyclic as well as heterocyclic compounds of biological significance. The reactions are usually catalyzed by using bases such as piperidine, pyridine and ammonia or sodium ethoxide in organic solvents, ammonia in organic solvents and the amino acids glycine **[15-20]**. The Knoevenagel condensation is also carried out by using $Zr(OPOK)_2$ **[21]**, natural phosphates such as NP doped with KF or NP/$NaNO_3$ **[22]**, synthetic phosphates like $Ca_2P_2O_7$ **[23]**, $K_2NiP_2O_7$ **[24]** and porous calcium hydroxyapatite **[11]** as catalysts. However, these methods required prolonged reaction time, high reaction temperature, toxicity, low recovery and use of costly catalysts. Therefore, introduction of clean procedures and utilizing eco-friendly green catalyst have attracted attention of researcher. In this regard we have used excellent green efficient catalyst in Knoevenagel condensation reaction by involving aromatic aldehydes with malononitrile. To the best of our knowledge, the reaction of various aromatic benzaldehydes with malononitrile is reported for the first time by using Ni NPs as catalyst in Knoevenagel condensation.

Nonetheless, the literature survey reveals that by using protective agents it enhanced the catalytic properties, antimicrobial activity and control particle shape of metal nanoparticles. The protection of metal nanoparticles surface could be achieved by coating, which can be done by various capping agent likes dicarboxylic acid **[25, 26]**, polyvinyl pyrrolidone and dodecylamine **[27]**, and epoxides **[28, 29]**. In our previous work [**30, 31**], we synthesized metal and metal oxides nanoparticles by using protective agents. In that respect, we have synthesized nickel nanoparticles by using ethylenediamine as protective agents and check out its catalytic and antibacterial activities. We found out an efficient and reusability of Ni NPs towards solvent free Knoevenagel condensation. The catalyst was found to exhibit an excellent recyclability and reusability (up to 4 times) without any additional treatment. Furthermore, the antibacterial activity of sample was carried out against bacterial pathogens. Meanwhile, their antibacterial activity analyzed after treatment of sonication. The study reveals Ni NPs shows strong effective toxicity against bacterial pathogens under sonication. To the best of our knowledge, antimicrobial activity of Ni NPs under sonication is also reported for the first time by agar well diffusion method.

## Experimental

*Materials and methods*

All the chemicals and solvents were used without further purifications. They includes Nickel nitrate hexahydrate (Sigma Aldrich), Ethylene glycol (Merck), Ethylenediamine (Merck), Hydrazine hydrate 80% (Sd Fine), Aromatic aldehydes (Merck), Malononitrile (Merck) and Ethyl acetate (Merck). Further, various pathogens used for antibacterial activity which were obtained from the Pathology and Diagnosis Laboratory Department of Microbiology, S. K. Porwal College, Kamptee (India). The strains and stock cultures were maintained at 4°C on nutrient agar.

*Agar well diffusion method*

The antibacterial activity of the nickel nanoparticles was performed by using well diffusion method **[32]**. About 20 ml of sterile molten Muller Hinton agar (HiMedia Laboratories Pvt. Limited, Mumbai, India) was poured into sterile petriplates. Triplicates plates were swabbed with the overnight culture ($10^8$ cells/mL) of pathogenic bacteria viz. *Staphylococcus aureus*, *Pseudomonas aeruginosa*, *Enterococcus faecalis*, *Escherichia coli*, and *Klebsiella sp*. Wells of size 6 mm have been made on Muller-Hinton agar plates using gel puncture. Finally, the nanoparticles samples dissolved in DMSO (20, 50, 60 µg/ml) were added from the stock into each well and incubated for 24 h at 37±2 °C. After 24 hour the zone of inhibition was measured and expressed as millimeter in diameter.

*Minimum inhibitory concentration (MIC)*

About 500 µl of different concentrations (2.5, 5, 10, 15 and 20 µg/ml) of nanoparticles were suspended in dimethylsulphoxide (DMSO) and samples were treated with ultrasonication with specific energy of 50 $x10^{-3}$ KHz for 10 minutes so that soft agglomerates were broken down into smaller nanoparticles and were mixed with 450 µl of nutrient broth which grow 50 µl of 24h old bacterial inoculums and allowed to grow overnight at 37 °C for 48 h. Nutrient broth alone served as negative control. The MIC was the lowest concentration of the nanoparticles that did not permit any visible growth of bacteria during 24 h of incubation on the basis of turbidity **[33]**.

*Spectroscopic and microscopic measurements*

The size and morphology of nickel nanoparticles were examined by JEOL model JSM-690LV, Scanning Electron Microscopy whose maximum magnification is 300,000X and resolution is 3nm at the Sophisticated Test and Instrumentation Center, Cochin University Kerala. TEM images were formed using CM200 which can produce magnification details up to 1,000,000X with resolution better than 10 A° at Indian Institute of Technology Pawai, Mumbai. The qualitative elemental analysis of the powder sample was studied by JEOL Model JED-200, Energy Dispersive Spectroscopy (EDS) and thermal analyses (TG/DTG/DTA) at heating rate 10 °C/min under nitrogen atmosphere at the Sophisticated Test and Instrumentation Center, Cochin University Kerala. The crystal structure of the sample was characterized by PXRD, Bruker AXS D8 Advance X-ray diffractometer using CuKα radiation. Infrared spectroscopy was recorded at a 2 $cm^{-1}$ resolution from 4000 to 400 $cm^{-1}$ on a Bruker IFS 66v Fourier transform spectrometer using KBr pellets. $^1$H-NMR was carried out NMR Spectrometer model Avance-II (Bruker) is the acquisition in the SAIF Chandigarh, India. The

 

instrument is equipped with a cryomagnet of field strength 9.4 T. Its $^1$H frequency is 400 Mhz. Mass analyses organic derivatives were carried out by expression CMS Mass Spectrometer at Synzel laboratory Gandhinagar, (India).

*Preparation of Ni NPs*

The Ni NPs were prepared by dissolving 0.1M nickel nitrate in 20.0 mL of ethylene glycol in 250 mL round flask and then 1.0 mL ethylenediamine was added to this solution. The system was maintained at room temperature, then the mixture was heated to 80 °C and reduced with 5 mL hydrazine hydrate (80 %) followed by 1.052 g of sodium hydroxide was added into the heated solution to enhance the reducing power. The grey color particles were separated by centrifugation (5250 rpm, 15 min) and then washed with several times with methanol, distilled water and acetone to remove the reducing agents. Nanoparticles were obtained after centrifugation kept in vacuum oven at 30 °C for drying. Further, characterizations of nickel nano catalysts were carried out by PXRD (**Fig. 1**), EDS (**Fig. 2**), FTIR spectra (**Fig. 3**), UV- visible spectra (**Fig. 4**), TG/DTG (**Fig. 5**), TEM (**Fig. 6**) and SEM (**Fig. 7**) in order to determine their formation, size and morphology behaviors.

*General procedure for the Knoevenagel condensation by Ni NPs under solvent-free condition*

In typical reaction procedure aldehydes (1 mmol) and malononitrile (1.2 mmol) were taken in a 25 ml round bottomed flask, then 0.01 g nickel NPs was added and was stirred on magnetic stirrer at 70 °C. The reaction progress was followed by TLC using n-hexane/ ethyl acetate (8:2) as eluent. After the completion of the reaction 15 ml of ethyl acetate was added to the reaction mixture, and the catalyst was separated by filtration and evaporated under reduced pressure to leave solid, which was recystallized from ethanol. Nanoparticles were recovered by centrifuging the aqueous layer and reutilized four times for the same reaction. The obtained products were characterized by various spectroscopy techniques such as $^1$H NMR, FTIR and Mass analyses, and then compared with authentic samples in the literature.

*Spectral data*

Selected data for typical compounds are given below.

**1.** 2-(2-chlorophenylmethylene) malononitrile (**Table 1**, **3a**). White solid, M.p. 92.0-93.0 °C, (literature m.p. 94-95.0 °C **[34]**), $^1$H NMR(DMSO $d_6$/TMS): $\delta$ = 8.56 (s, 1H, CH), 8.06-7.52 (m, 4H, ArH), FTIR (KBr, $\nu$/cm$^{-1}$): 3047, 2221, 1638, 1583, 1129, 755; m/z =212 $[M^+ + Na]^+$.

**2.** 2-(4-hydroxyphenylmethylene) malononitrile (**Table 1**, **3d**). Yellow solid, M.p. 148.0-150.0 °C, (literature m.p. 152 $^0$C **[34]**), $^1$HNMR (DMSO $d_6$/TMS): $\delta$ =11.03 (s, 1H, OH), 8.13 (s, 1H, CH), 7.88-6.95, (s, 4H, ArH), IR (KBr, $\nu$/cm$^{-1}$): 3672, 3363, 3028, 2222, 1610, 1569, 1569, 859, MS(ESI), m/z =193 $[M^+ + Na]^+$.

**3.** 2-(phenyl methylene) malononitrile (**Table 1**, **3f**). White solid, M.p. 80.0-81.0 °C, (literature M.p. 83.5–84.0 °C **[34]**), $^1$H NMR (DMSO $d_6$/TMS): $\delta$ = 8.41 (s, 1H, CH), 7.88-7.74 (m, 5H, ArH), IR (KBr, $\nu$/cm$^{-1}$) 3013, 2223, 1675, 1163, 755 MS(ESI), m/z =187 $[M^+ + Na]^+$.

**4.** 2-(4-nitrophenylmethylene) malononitrile (**Table 1**, **3j**). Yellow solid, M.p. 161-162°C, (literature M.p. 161 $^o$C **[34]**), $^1$HNMR(DMSO $d_6$/TMS): $\delta$ = 8.71 (s, 1H, CH), 8.41-8.16 (M, 4H, ArH), IR (KBr, $\nu$/cm$^{-1}$) 3038, 2230, 1636, 1579, 1070, 831 m/z =222 $[M^+ + Na]^+$.

## Results and discussion

There are various numbers of methods available for the production of Ni NPs such as conventional polyol process, spray-pyrolysis method, chemical/electrochemical methods and microwave plasma deposition. Among the chemical synthetic methods modified polyol method is more suitable for the production of Ni NPs. Therefore, this method is widely accepted by various researchers. However, the synthesis of Ni NPs by using capping agents or protective agents is an interesting work, which enhanced the novel properties of nanoparticles viz. catalytic, microbial activity and also controls the sizes of metal at nano level. Very less work has been done on Ni NPs by using capping agents. Hence, we choose this technique for the production of Ni NPs by taking ethylenediamine (en) as protective agents having excellent catalytic properties and high stability **[11]**. The nickel nitrate was reduced with hydrazine hydrate in the presence of ethylenediamine as structure-directing agent in ethylene glycol (Reaction I) which lead to the formation of highly monodisperse nickel nanoparticles **[33]**. The reduction reaction could be expressed as,

$$2\,Ni^{2+} + N_2H_2 + 4OH^- \xrightarrow{\text{en}} 2\,Ni + N_2 + 4\,H_2O \quad \text{(Reaction I)}$$

Further, we paid much more attention for synthesis of organic compounds by using Ni NPs as catalyst in Knoevenagel condensation. The Knoevenagel condensation is one of the most useful and widely accepted methods for organic synthesis with numerous applications in the synthesis of fine chemicals. Recently, tremendous works have been done on Knoevenagel condensation of aromatic aldehydes with malononitrile by using some bases but none of work was carried out by using Ni NPs as catalyst. Therefore, in an effort to find out an alternative method for Knoevenagel condensation reaction, we used Ni NPs as catalyst. Herein, we have reported a simple easy and convenient protocol for production of various aromatic organic compounds (3a-l) by the reaction of aromatic benzaldehyde (1a-l) with malononitrile (2) utilizing Ni NPs as catalyst (Reaction II). In general procedure for the Knoevenagel condensation by using Ni NPs under solvent-free condition is given in experimental section. The products were obtained in short time with high yield having remarkable catalytic activity, ecofreindly and recoverability of Ni NPs.

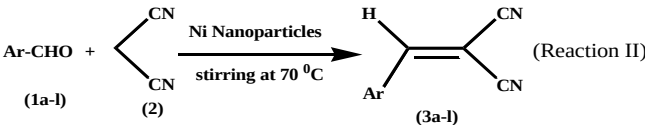

(Reaction II)

Apart from novel catalytic property of Ni NPs, sample was tested against various bacterial pathogens under without sonication and after treatments with sonication. Overwhelming antimicrobial results were obtained against pathogens in sonication treatment; this reveals Ni NPs are good antibacterial agents. literary survey suggest that, there are very few less work has been done on Ni NPs as antibacterial agents, however none of antibacterial work was published earlier under sonication. Therefore, the catalytic and antibacterial properties of Ni NPs would be a novel work in the present investigation. In an effort to find out scaffold and outstanding properties and stability of nickel nanoparticles were characterized by various microscopic spectroscopic techniques while performing its catalytic and antimicrobial activities.

*Characterization and stabilization of Ni NPs*

The synthesized Ni NPs were characterized by various spectroscopic techniques in order to validate its formation and their size in nano scale. The formation of Ni NPs was primarily confirmed from the powder X-ray diffraction (PXRD) curve (**Fig. 1**) and energy dispersive spectrum (EDS) (**Fig. 2**). From **Fig. 1** it can be seen that the PXRD pattern exhibits three sharp diffraction peaks at 2θ=44.5°, 51.8°, 76.4°, correspond to the (1 1 1), (2 0 0) and (2 2 0) planes of pure face-centered cubic (fcc) respectively, which is according to a standard JCPDS card (No. 04-0850). Further, average particle size of the Ni NPs was calculated from the major diffraction peak (1 1 1) using the Debye-Scherrer equation and it was to be above 6 nm. No evident peaks were detected for nickel oxide or hydride. Therefore, PXRD pattern noteworthy supports for formation of nickel nanoparticles.

$$D = \frac{K\lambda}{\beta cos\theta}$$

where, K is a constant equal to 0·89, λ the X-ray wavelength (λ=0·154095 nm), β the full wavelength at half maximum, θ the half diffraction angle, D is the particle diameter size.

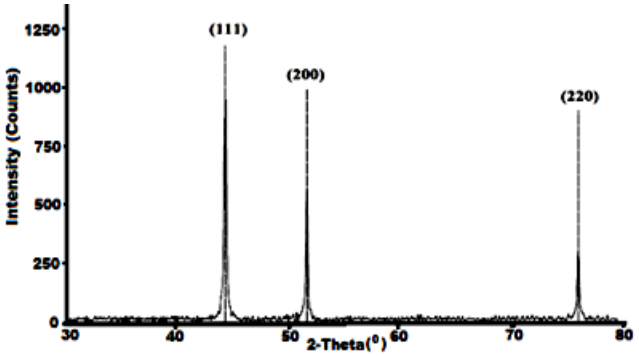


**Fig. 1.** PXRD diffraction pattern of Ni NPs.

Furthermore, in order to confirm the presence of an element in a sample EDS analysis was carried out and has been displayed in **Fig. 2**. The elemental analyses of Ni-NPs were performed through EDS which showed the relative intensity of the Ni, $O_2$, and carbon. The presence of $O_2$ and carbon could be attributed to the existence of unknown form of carbonaceous organic residue against interpret. Further, Fourier transform infrared spectroscopy (FTIR, Bruker IFS 66V/S) was used to study the chemical affinity of the sample towards the surface of the nanoparticles and spectrum of nanoparticles has been shown in **Fig. 3**. From, the FTIR spectrum (**Fig. 3**) indicated that no strong peaks were obtained for any functional group of metal nanoparticles prepared by modified polyol process. However, some very weak peaks were observed in **Fig. 3** due the carbaneous moiety together with nanoparticles.

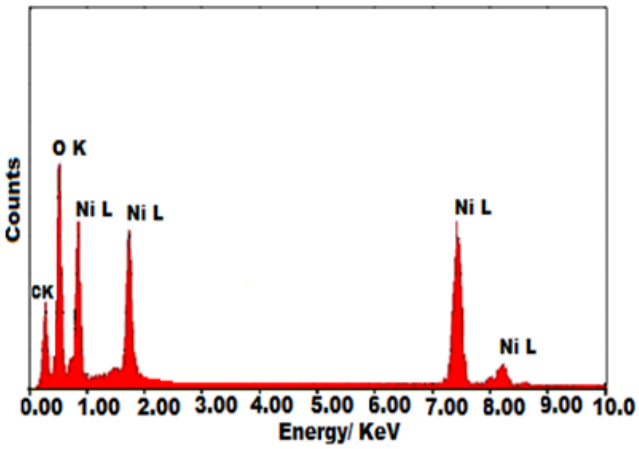


**Fig. 2.** EDS spectrum of Ni NPs sample.

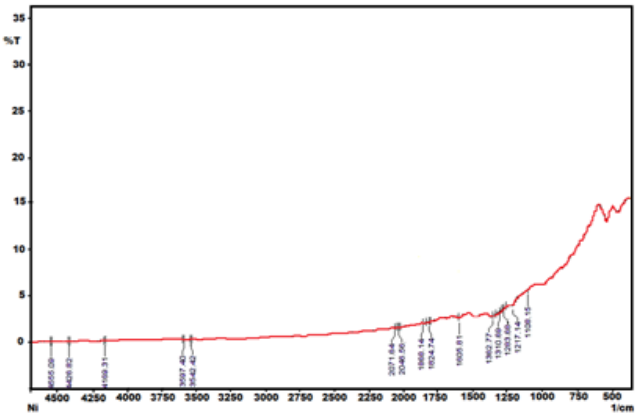


**Fig. 3.** FT-IR spectrum of synthesized Ni NPs.

The obtained peaks around 4555, 4426, 4169 and 3542 $cm^{-1}$ were may be due to the air, water or $CO_2$ background **[36, 37]**. The peak which was seen at range 550-500 may be due to the metal nature **[37]**. However, weak peaks were seen in FT-IR spectrum at range 4100-2100 $cm^{-1}$ due to the C-H and N-H stretching of ethylenediamine which might have binded to nickel as protective agent. Additionally, the metallic nature of nanoparticles was confirmed by UV-visible spectral data whose broad peaks displayed to the range 250-70 nm **[38]** and are shown in **Fig. 4**. Therefore, UV-visible electronic curve could not be assigned to either nitrate of nickel salt or any organic ligand attached with metal atom. Hence, FTIR and UV spectra did not give any proper evidence for any organic moiety however it was assumed that the presence of a carbonaceous organic residue which may be resulted from presence of protective or capping agents. Nonetheless, such ambiguity

 

interpretation was reported by Leonard *et al.* on formation of an unknown carbonaceous organic residue during synthesis of PtNi intermetallic nanoparticles. From pertaining this view to identify the carbonaceous organic moiety, the sample was further investigated by thermogravimetric analysis. In the present work, the thermogravimetric analysis (TG) is supported by differential thermal analysis (DTA) and derivative thermogravimetry (DTG).

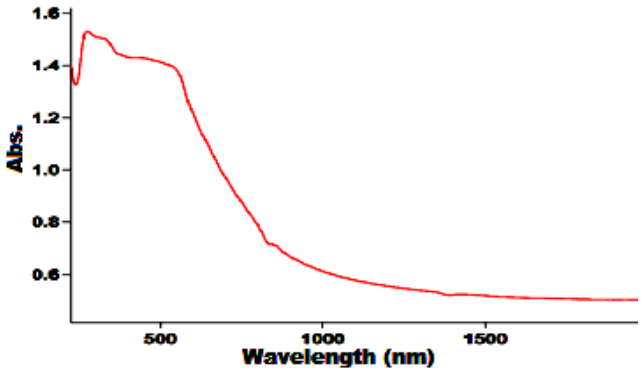


**Fig. 4.** UV-Visible spectrum of Ni NPs.

These techniques are widely used to evaluate the thermal degradation behaviour and the thermal stability of carbonaceous organic moiety in compounds **[37, 39, 40,]**. TG/DTG curve of nanoparticles are presented in **Fig. 5**. In **Fig. 5** it is observed that the sequence of degradation that takes place in Ni NPs starts with dehydration of adsorbed water molecules followed by the release of organic fragments of the backbone. This seems like a multistage decomposition process *i.e.* thermal decomposition profile which occurs through two to three steps. The initial steps of degradation at 39.77°C - 200 ºC associated with broad $T_{DTG}$ peak at 101 °C that may be correspond to the removal of lattice water. **Fig. 5** also suggests that the mass loss in range 200-730 °C associated with two broad $T_{DTG}$ peaks at 273 °C and 355 °C. In the second and third stages this might be due to the degradation of organic residue which attached on surface of nanoparticles. From above discussed studies, it can be explained that the surface bound carbonaceous moiety to Ni NPs is from the surface oxidation. As soon as the organic moiety loss, there was no further loss of weight probably which may be due to the Ni metal formation.

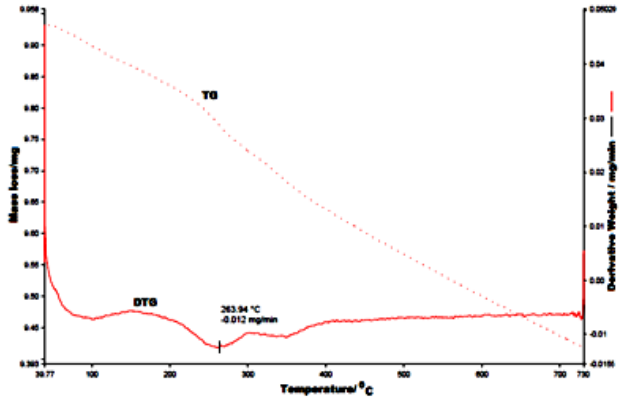


**Fig. 5.** TG/DTG curve of Ni NPs.

*Microscopic investigation*

Nonetheless, the size and morphological behavior of the Ni NPs were observed by transmission electron microscopy (TEM) (**Fig. 6**) and scanning electron microscopy (SEM) technique (Fig. A-D). In **Fig. 7**, the products are look like globular and spherical shape with the sizes in the range 20-200 nm. The nanoparticles products were observed ball-shape aggregates with distinct diameters. Those individual particles possibly further grow to form a long chain of balls or stack of balls. The two different sizes spherical shape particles were bounded to each other by some forces with amorphous surface of organic residue. Also, it was supported by PXRD technique. The size measured from PXRD data using Debye-Scherrer equation was within the range which could be obtained from the transmission electron microscopy images. **Fig. 7A-D** clearly display that the particles are bounded with an amorphous surface of organic residue which might be due to presence of protective agent ethylenediamine. Also, the presence of carbaneous body on Ni NPs was clearly seen by TEM. The TEM image suggests the presence of (1 1 1) plane of fcc Ni and selected area electron diffraction pattern (SAED) shows a ring pattern corresponding to all planes of the fcc Ni (**Fig. 6A**). Hence, it likely to argument that the TEM images are noteworthy supported with SEM results. Apart from this, the elemental analysis (EDS), and UV-visible spectroscopy (**Fig 5**) were noteworthy supported for the existence of Ni (0) NPs. The EDS analyses (**Fig 2**) shows relative intensity of oxygen and carbon which might be due to the unknown form of carbonaceous organic residue as well as surface oxidation.

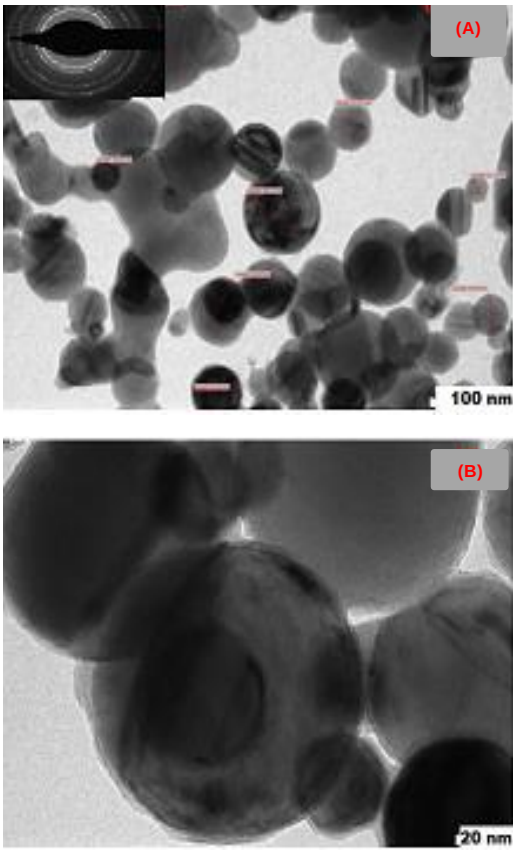


**Fig. 6.** TEM images (A and B) of Ni NPs.

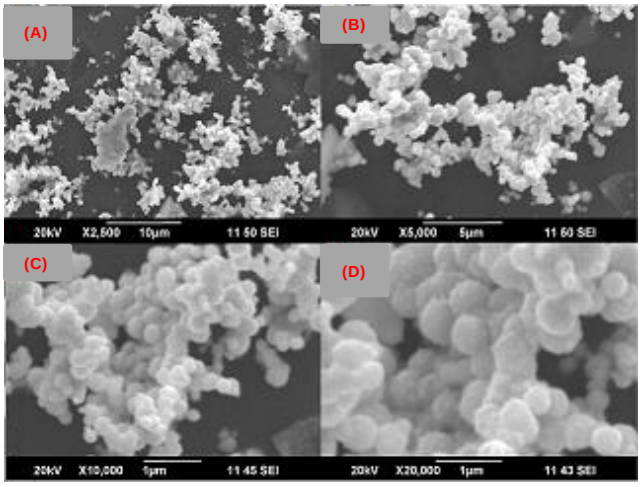


**Fig. 7.** SEM image (A, B, C and D) of Nickel NPs.

*Catalytic property of Ni NPs*

Herein, we have reported a simple, easy and convenient protocol for the solvent-free Knoevenagel condensation between aromatic benzaldehyde and malononitrile catalyzed efficiently by Ni NPs. It's an evident that the electron rich, the electron deficient compounds reacted smoothly with heterocyclic benzaldehyde which produced high yield of product. The results of different aromatic aldehydes have been summarized in **Table 1**.

**Table 1.** Ni NPs catalyzed Knoevenagel condensation of various aromatic aldehydes with malononitrile.

| Products[a] | Ar | Time (min) | Yields[b] (%) | Color | Found | Literature |
|---|---|---|---|---|---|---|
| 3a | 2-$ClC_6H_4$ | 30 | 90 | White | 92-93 | 92[a] |
| 3b | 3-$OHC_6H_4$ | 47 | 89 | Yellowis | 148-150 | 152[b] |
| 3c | 4-$ClC_6H_4$ | 45 | 95 | Brown | 161-162 | 162[a] |
| 3d | 4-$OHC_6H_4$ | 50 | 96 | Yellow | 185-186 | 188[a] |
| 3e | 2-$NO_2C_6H_4$ | 65 | 88 | Yellow | 120 | 138[a] |
| 3f | $C_6H_5$ | 45 | 95 | White | 80-81 | 82[a] |
| 3g | 3-$BrC_6H_4$ | 46 | 86 | White | 155-156 | 155[a] |
| 3f | 2-Furyl | 53 | 86 | Whitish yellow | 70-71 | 72[a] |
| 3i | 3-$NO_2C_6H_4$ | 63 | 90 | White | 103-104 | 103[a] |
| 3j | 4-$NO_2C_6H_4$ | 45 | 90 | Yellow | 161-162 | 161[a] |
| 3k | 4-OCH3C6H5 | 50 | 89 | Yellow | 110-112 | 113[a] |
| 3l | $C_6H_5CH$=CH | 45 | 87 | white | 125-126 | 128[a] |

[a]Some products were characterized (IR,1H NMR and MS) data and compared with authentic samples and [b] isolated yields.

In this case to determine the appropriate concentration of the Ni NPs catalyst for Knoevenagel condensation we have investigated the model reaction of benzaldehyde, and malononitrile at different concentrations. We found out the organic products 40 %, 47 %, 64 %, 85 %, 95 %, and 95 % at 2, 4, 6, 8, 10, and 12 mol % concentrations of Ni NPs respectively. Hence, this reveals that at10 mol % Ni NPs produces the best results with respect to product yield. The series of Knoevenagel condensation were displayed by applying the method mentioned above (experimental section). We also found out that the aromatic aldehydes containing different functional group at different position work well and did not show in the product's yield. Interestingly, we have noteworthy examined the recovery and reuse of the catalyst after product's formations. The catalyst were recovered by a simple work-up using centrifugation method and reused during four consecutive runs by apparent loss of reactivity only 2 % for the same reaction. Conceivable mechanisms for the formation of the products (3a-l) have been shown in **Scheme 1**. The more important is that Ni NPs facilitate the Knoevenagel-type coupling by coordinated to the oxygen of carbonyl groups. On the other hand, Ni NPs can activate methylene compounds *i.e.* malononitrile so that deprotonation of the C-H bond occurs. As a result Knoevenagel condensation proceeds by activation of reactants by NPs.

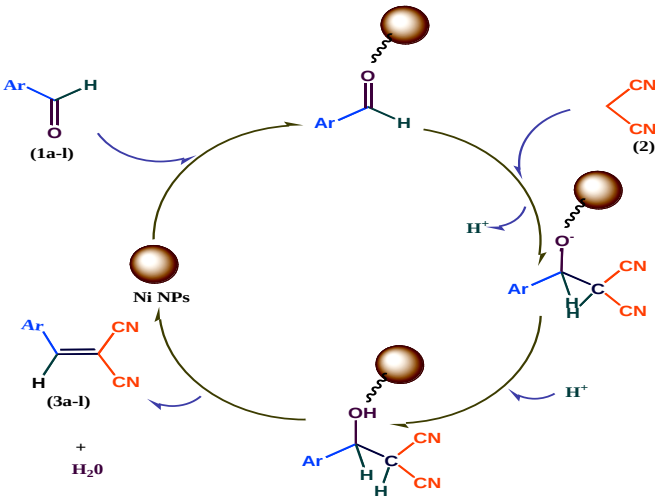


**Scheme 1.** The proposed mechanism for Knoevenagel condensation by Ni NPs.

*Reusability of the Ni NPs catalyst*

In order to investigate the reusability of the catalyst, 0.01 g nickel nanoparticles were used for condensation of 3-Nitrobenzaldehyde and malonitrile. After completion of reaction, catalyst were recycled and directly used for next cycle. The yield obtained by the recover catalyst decreases only by 2 %, however before three cycles there would be much more superior reusability of Ni NPs. The comparative recyclability and yield of Ni NPs catalyst in Knoevenagel condensation has been shown in **Fig. 8**.

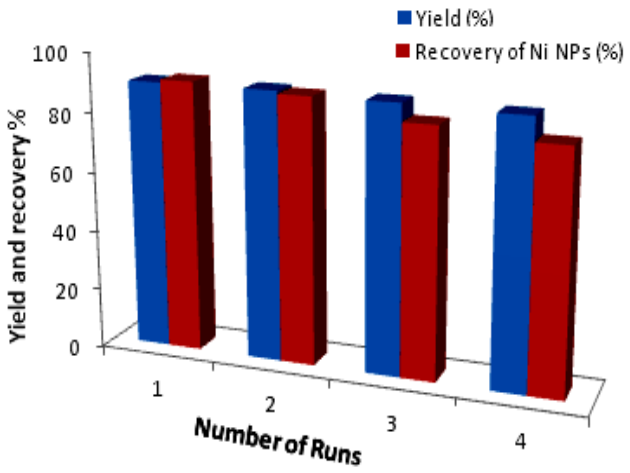


**Fig. 8.** Recyclability of Ni NPs catalyst in Knoevenagel condensation.

*Antibacterial activity of Ni NPs*

The antimicrobial activity of Ni NPs in different concentration (20-60 µg) was quantitatively assessed on the basis of zone of inhibition and compared with standard antibiotic accordance to the reference methods of the Clinical and Laboratory Standards Institute (CLSI) **[41]** (**Table 2**). Among the Gram negative bacteria tested, *Pseudomonas araginosa* not only shows strong inhibition by nickel nanoparticles at higher concentration (21 mm) but also at low concentration (17 mm). Similarly, *Klebsiella sp*. (20 mm) and *E.coli* (18 mm) were moderately inhibited by Ni NPs. Besides, Gram positive bacteria were tested like *Staphylococcus aureus* (21mm) exhibited a maximum zone of inhibition at 60 µg of Ni NPs. The present study suggested that Ni NPs exhibited a strong antibacterial activity against all the test pathogens even at lower concentration. Antibacterial activity of Ni NPs sample after treatment with sonication against different pathogens have shown in **Fig. 9**.

**Table 2.** Zone of inhibition of synthesized Ni NPs is against various pathogenic bacteria.

| Zone of inhibition µg (mm) against pathogenic bacteria | | | | | | | | | | | | |
|---|---|---|---|---|---|---|---|---|---|---|---|---|
| Ni NPs | *Staphylococcus aureus* | | | *Pseudomonas aeruginosa* | | | *Escherichia coli* | | | *Klebsiella sp.* | | |
| | 20µg | 40 µg | 60 µg | 20 µg | 40 µg | 60 µg | 20 µg | 40 µg | 60 µg | 20 µg | 40 µg | 60 µg |
| | 14 | 17 | 21 | 14 | 17 | 21 | 14 | 16 | 18 | 11 | 13 | 20 |
| Standard Antibiotic | | | | | | | | | | | | |
| Amikacin (AK) 30mcg | 14 mm | | | 15mm | | | 19mm | | | 21mm | | |
| Ciprofloxacin (CF) 5mcg | 34 mm | | | 27 mm | | | 26mm | | | 29 mm | | |
| Gentamicin (G) 30mcg | 15 mm | | | 16 mm | | | 17 mm | | | 18 mm | | |
| Norfloxacin (Nx) 10mcg | 30 mm | | | 24 mm | | | 23 mm | | | 27 mm | | |

Meanwhile, on comparing the effect of standard antibiotics among the tested pathogens, it was found that *Pseudomonas aeruginosa* exhibits resistance to *Amikacin* and *Gentamicin*, but inhibited by *Norfloxacin* (24 mm) (**Table 2**). Similarly, *Staphylococcus aureus* exhibited high sensitivity against *Norloxacin* (30 mm), but minimum zone of inhibition obtained against *Amikacin* and *Gentamicin*. This shows that even the *Amikacin* and *Gentamicin* resistant *Pseudomonas aeruginosa* was strongly inhibited by Ni NPs at concentration (40 µg).

Furthermore, the MIC study revealed that the Ni NPs showed sensitivity at the conc. of 10 µg/ml, against *E. coli* and *Klebsiella sp.* and *Pseudomonas aruginosa* 15 µg/ml and 15 µg/ml against *Staphylococcus aureus*. The Ni NPs showed much higher activity against *Pseudomonas aruginosa* than against *Staphylococcus aureus* before sonication. The higher deactivation efficiency in the case of gram-negative bacteria as compared to gram-positive ones was reported earlier **[42, 43]**. This difference can be attributed to the differences in the cell wall structure inherent in gram-negative and gram-positive bacteria. Gram-positive and Gram-negative bacteria have similar internal, but very different external structures. A gram-positive bacterium has a thick peptidoglycan layer that contains teichoic and lipoteichoic acids. A gram-negative bacterium has a thin peptidoglycan layer and an outer membrane that contains lipopolysaccharide, phospholipids, and proteins. This permits a conclusion that the bacteria antimicrobial rate is governed not only by cell wall thickness, but also by the morphology of cell envelop and resistance of outer membrane to the reactive oxygen species produced at the photocatalyst surface. Moreover, we were found 50 x $10^{-3}$ khz for 10 minutes result of sonication in order to get the particle size reduction, and which was depend on the applied energy per volume of the dispersion (specific energy) **[44, 45]**. As the specific energy applied on samples then increases two fold antimicrobial activity in our experiment.

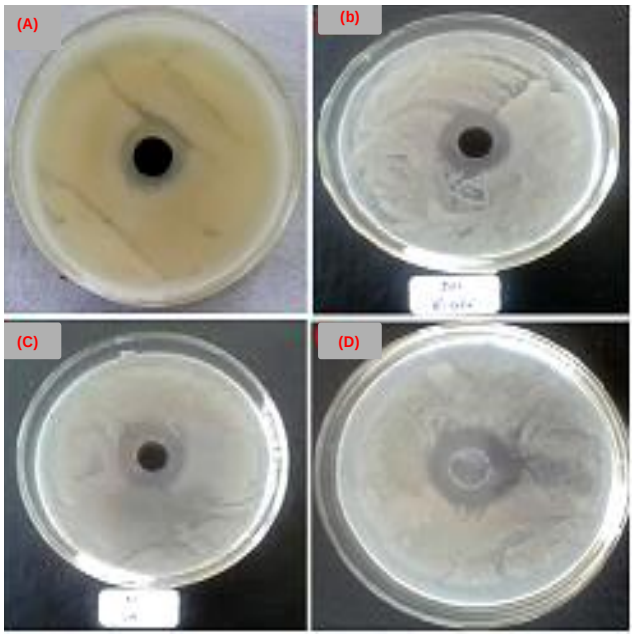


**Fig. 9.** Antibacterial activity of Ni NPs sample after treatment with sonication against (A) *Pseudomonas araginosa*, (B) *E. coli*, (C) *Staphylococcus aureus* and (D) *Klebsiella sp.*

The overall charge of bacterial cell at biological pH values is negative because of excess number of carboxylic groups, which upon dissociation make the cell surface negative. The opposite charges of bacteria and nanoparticles are attributed for their adhesion and bioactivity due to the electrostatic forces.

It is logical to state that binding of the nanoparticles to the bacteria depend on the surface area available for interaction. Nanoparticles have large surface area available for interactions which enhances bactericidal effect than the large sized particles; hence they impart cytotoxicity to the microorganisms **[46]**.

The mechanism by which the nanoparticles penetrates into bacteria is not understood completely, but studies suggest that when *E. Coli* was treated with nickel, changes took place in its membrane morphology and produced a significant increase in its permeability affecting proper transport through the plasma membrane, leaving the bacterial cells incapable of properly regulating transport through the plasma membrane, resulting into cell death. It was observed that Nickel nanoparticles have penetrated

inside the bacteria and believed to have caused damage by interacting with phosphorous and sulphur containing compounds such as DNA **[47]**. Nickel tends to have a high affinity to react with such compounds. The possible mechanism of action of Ni NPs is considered that DNA may have lost its replication ability and cellular proteins become an inactive after treatment. Another reason would be the release of Ni ions from nanoparticles, which will have an additional contribution to the bactericidal efficiency of Nickel nanoparticles.

Heavy metals are toxic and reactive with proteins; therefore, they bind protein molecules; as a result cellular metabolism is inhibited causing death of microorganism. It is believed that Nickel nanoparticles after penetration into bacteria inactive their enzymes, generate hydrogen peroxide and cause bacterial cell death **[48]**. Furthermore, experimental observations have explained significantly the antibacterial behaviour of Nickel nanoparticles. When *E. coli* was treated with highly reactive metal nanoparticles, an inhibitory effect has taken place **[49]**. Ni nanoparticles after adherence to the surface of the cell membrane distributed its respiration as $Ni^{2+}$ interact with enzymes of the respiratory chains of bacteria **[50]**. Metal depletion caused formation of irregular shaped pits in the outer membrane of bacteria which is caused by progressive release of LPS molecules and membrane proteins **[51]**. In addition, it is believed that Nickel binds to functional groups of proteins, resulting in protein denaturation **[52]**. As observed, bacterial growth log phase has a delayed trend at lower concentrations of Ni NPs loadings. Therefore, it was concluded that complete bacterial inhibition depends upon the concentrations of NPs and on the number of bacterial cells. Indeed, it reflects that Ni NPs have significant biocide effect in reducing bacterial growth for practical applications.

## Conclusion

In conclusion, we have successfully synthesized Ni NPs by chemical reduction method using ethylenediamine as protecting agent and characterized by various spectroscopic and microscopic techniques for particle size and morphology. Further we have demonstrated the first time Ni NPs as potential alternative of novel-metal-based catalysts for Knoevenagel condensation. In the present investigation synthesized aromatic compounds by stirring at 70 °C that provides an efficient and very simple solvent-free method for the Knoevenagel condensation *via* benzaldehyde and malononitrile using Ni NPs as a catalyst. This catalyst was expected to contribute to the development of more environment-benign methods and forms part of nano-metal chemistry. The mildness of the conversion, experimental simplicity, compatibility with various functional groups, excellent yields, shorter reaction time, and the easy work-up procedure makes this procedure more attractive in synthesizing a variety of these derivatives.

Moreover, antibacterial properties of nickel nanoparticles were carried out very successfully on human bacterial pathogens. The zones of inhibition were formed in the antimicrobial screening test indicated that the Ni NPs synthesized in this process has an efficient antimicrobial activity against pathogenic bacteria. Thus synthesized Ni NPs can be used in medical field due to their efficient antimicrobial function.

**Acknowledgements**

This work was supported by Science and Engineering Research Board (SERB), New Delhi (India). R.G. C gratefully acknowledge to funding department SERB for awarding Major Research Project, Grant No. SB/EMEQ-366/2014. Also, acknowledge to IIT Mumbai, STIC Cochin, SAIF Chandigarh and SYNZEL Gandhinagar for their valuable spectral analyses.

**Reference**

1. Rodriguez-Leon, E.; Iniguez-Palomares, R.; Navarro, R.; Herrra-Urbina, R.; Tanori, J.; Palomares, C.; Maldonado, A.; *Nano Res. Lett.*, **2013,** *8*, 318. **DOI**:10.1186/1556-276X-8-318
2. Dominguez-Crespo, M.; Ramirez-Meneses, E.; Montiel-Palma, V.; Torres Huertaa, A.; Dorantes Rosalesc, H.; *Int. J. Hydr. Enen*, **2009**, *34*, 1664. **DOI**: 10.1016/j.ijhydene.2008.12.012
3. Wang, Y.; Gunasekaran, S.; *J. Nanopart. Res*; **2011**, *14*, 1200. **DOI**: 10.1007/s11051-012-1200-2
4. Cordente, N.; Respaud, M.; Senocq, F.; Casanove, M.; Amiens, C; Chaudret, B; *Nano Letts*. **2001**, *1*, 565. **DOI:** 10.1021/nl0100522
5. Mirkin, C.; Letsinger, R.; Mucic, R.; Storhoff, J.; *Nature* **1996**, *382*, 607. **DOI**:10.1038/382607a0
6. Storhoff, J.; Elghanian, R.; Mucic, R.; Mirkin, C.; Letsinger, R.; *J. Am. Chem. Soc*. **1998,** *120*, 1959. **DOI:** 10.1021/ja972332i
7. Morozov, Y.; Belousova, O.; Kuznetsov, M.; *Inorg. Mater*. **2011,** *47*, 36. **DOI**: 10.1134/S0020168510121027
8. Saxena, A.; Kumar, A.; Mozumdar, S.; *J. Molec. Cataly. A: Chemic*. **2007**, *269*, 35. **DOI:**10.1016/j.molcata.12.042
9. Khurana, J.; Vij, K.; *J. Chem. Sci.* **2012,** *124*, 907. **DOI**:10.1007/s12039-012-0275-8
10. Jiang, Z.; Xie, J.; Jiang, D.; Wei, X.; Chen, M.; *Cryst. Eng. Comm*, **2013** *15*, 560. **DOI**: 10.1039/c2ce26398j
11. Sapkal, S.; Shelke, K.; Shingate, B.; Shingare, M.; *Tetrahed. Letts.* **2009,** *50*, 1754. **DOI:** 10.1016/j.tetlet.2009.01.140
12. Olyaei, A.; Vaziri, M.; Razeghi, R.; Shams, B.; Bagheri, H.; *J. Serb. Chem. Soc*. **2013**, *78*, 463. **DOI**: 10.2298/JSC120506076
13. Dhakshinamoorthy, A.; Pitchumani, K.; *Tetrahedr. Letts.* **2008,** *49*, 1818. **DOI**: 10.1016/j.tetlet.2008.01.061
14. Chou, K.; Huang, K.; *J. Nanopart. Res.* **2001**, *3*, 127. **DOI:** 10.1023/a:1017940804321
15. Rao, P.; Venkataratnam, R.; *Tetrahed. Lett.* **1991,** *32*, 5821. **DOI**: 10.1016/S0040-4039(00)93564-0
16. Pasha, M.; Manjula, K.; *J. Saudi. Chem. Soc*. **2011,** *15*, 283. **DOI**:10.1016/j.jscs.2010.10.010
17. G'ora, M.; Kozik, B.; Jamro'zy, K.; Luczy'nskim, K.; Brzuzan, P.; Wo'zny, M.; *Gree. Chem.* **2009,** *11*, 863. **DOI:** 10.1039/B820901D
18. Bennazha, J.; Zahouily, M.; Sebti, S.; Boukhari, A.; Holt, E.; *Catal. Commun.* **2000,** *2*, 101. **DOI**: 10.1016/S1566-7367(01)00015-2
19. Vinay Kumar, B.; Naik, H.; Girija, D.; Vijaya Kumar, B.; *J. Chem. Sci.* **2011**, *123*, 615. **DOI**:10.1007/s12039-011-0133-0
20. Thirupathi, G.; Venkatanarayana, M.; Dubey, P.; Bharathi Kumari, Y.; *Der Pharma. Chemica*. **2012**, *4*, 1897. **DOI**: 10.1155/2012/191584
21. Wang, Z.; Wangc, C.; Wang, H.; Zhang, H.; Su, Y.; Ji, T.; Wang, Lie.; *Chin. Chem. Letts*. **2014**, 25, 802. **DOI**: 10.1016/j.cclet.2014.03.036
22. Sebti, S.; Smahi, A.; Solhy, A.; *Tetrahed. Letts.* **2002,** *43*, 1813. **DOI:** 10.1016/S0040-4039(02)00092-8
23. Maadi, A.; Matthiesen, C.; Ershadi, P.; Baker, J.; Herron, D.; Holt,

 

E.; *J. Chem. Cryst.* **2003**, *33*, 757.
**DOI**: 10.1023/A:1026155323394
24. Mallouk, S.; Bougrin, K.; Laghzizil, A.; Benhida, R.; *Molecules* **2010**, *15*, 813.
**DOI:** 10.3390/molecules15020813
25. Jouet, R.; Warren, AD.; Rosenberg, D.; Bellitto, V.; Park, K.; Zachariah, M.; *Chem. Mater*. **2005**, *17*, 2987.
**DOI**: 10.1021/cm048264y
26. Fernado, S.; Smith, M.; Harruff, B.; Lewis, W.; Guliants, E.; Bunker, C.; *J. Phys. Chem. C.* **2009**, *113*, 500.
**DOI:**10.1021/jp809295e
27. Li, D.; Komarneni, S.; *J. Am. Ceram. Soc.* **2006**, *89*, 1510-1517.
**DOI**: 10.1111/j.1551-2916.2006.00925.x
28. Chung, SW.; Guliants, E.; Bunker, CE.; Hammerstroem, D.; Deng, Y.; Burgers, M.; Jelliss, P.; Buckner, S.; *Langmuir* **2009**, *25*, 8883.
**DOI:** 10.1021/la901822h
29. Hammerstroem, D.; Burgers, M.; Chung, S.; Guliants, E.; Bunker, C.; Wentz, K.; Hayes, S.; Buckner, S.; Jelliss, P.; *Inorg. Chem.* **2011**, *50*, 5054.
**DOI:**10.1021/ic2003386
30. Tanna, J.; Chaudhary, RG.; Juneja, HD.; Gandhare, NV.; Rai A.; *BioNanoSci*. **2015**, *5*, 123.
**DOI:** 10.1007/s12668-015-0170-0
31. Gandhare, NV Chaudhary, RG.; Meshram, VP.; Tanna, J.; Lade, S.; Gharpure, MP.; Juneja, HD.; Rai A.; *J. Chin. Adv. Mater. Soc.* **2015**, 1.
**DOI:**10.1080/22243682.2015.1068134
32. Salal, R.; Suchitra. *African J Micro Res*; **2009**, *3*, 97.
33. Hammond, S.; Lambert, P.; *London: Edward Arnld Ltd.*; **1987**, *8*.
34. Rong, L.; Han, H.; Jiang, H.; Tu, S.; *Int. J. Rapid. Comm. Synth. Org. Chem.* **2008**, *38*, 3530.
**DOI**: 10.1080/00397910802164724
35. Wu, X; Xing, W.; Zhang, L.; Zhuo, S.; Zhou, J.; Wang, G.; Qiao, S.; *Powder. Technol*. **2012**, *224*, 162.
**DOI**: 10.1016/j.powtec.2012.02.048
36. Ghanta, S.; Muralidharan, K.; *J. Nanopart. Res;* **2013**, *15*, 1715.
**DOI**:10.1007/s11051-013-1715-1
37. Leonard, B.; Zhou, Q.; Wu, D.; Di Salvo, F.; *Chem. Mater*. **2011**, *23*, 1136.
**DOI:** 10.1021/cm1024876
38. Chandra, S.; Kumar, A.; Tomar, P.; *J. Saudi Chem. Soc*. **2014**, *18*, 437.
**DOI:** 10.1016/j.jscs.2011.09.008
39. Chaudhary, R.; Juneja, H.; Gharpure, M.; *J. Therm. Anal. Calorim.* **2013**, *112*, 637.
**DOI**: 10.1007/s10973-012-2616-8
40. Chaudhary, R.; Juneja, H.; Pagadala, R.; Gandhare, N.; Gharpure, M.; *J. Saudi Chem. Soc.* **2014**, *19*, 442..
**DOI**: 10.1016/j.jscs.2014.06. 002
41. CLSI, Document.; *Clinical Laboratory Standards Institute, Wayne, PA. M2-A9*, **2006**, *26*, 1.
42. Rincon, A.; Pulgarin, C.; *Appl. Catal. B: Environ*. **2004**, *49*, 99.
**DOI:** 10.1016/j.apcatb.2003.11.013
43. Pal, A.; Pehkonen, S.; Yu, L.; Ray, M.; *J. Photochem. Photobiol. A. Chem.* **2007**, *186*, 335.
**DOI:** 10.1016/j.jphotochem.2006.09.002
44. Hielscher, T.; *Dans European Nano Systems Worshop - ENS* **2005**, *Paris: France.*
**DOI:** arXiv: 0708.1831
45. Pohl, M.; Hogekamp, S.; Hoffmann, N.; Schuchmann, H.; *Chemie Ingenieur Techni*. **2004**, *76***,** 392.
**DOI**: 10.1002/cite.200403371
46. Baker, C.; Pradhan, A.; Pakstis, L.; Darrin, J.; Ismat, S.; *J. Nanosci. Nanotechnol.* **2005**, *5*, 244.
**DOI**: 10.1166/jnn.2005.034
47. Elechiguerra, J.; Burt, J.; Morones, J.; *J. Nanobiotechnol*. **2005**, *3*, 1.
**DOI:** 10.1186/1477-3155-3-6
48. Kokkoris, M.; Trapalis, C.; Kossionides, S.; Vlastou, R.; Nsouli, B.; Grötzschel, R.; Spartalis, S.; Kordas, G.; Paradellis, T.; *Nucl. Instr. and Meth. Phys. Res. B.* **2002**, *188*, 67.
**DOI:** 10.1016/S0168-583X(01)01020-5
49. Stoimenov, P.; Klinger, R.; Marchin, G.; Klabunde, K.; *Langmuir* **2002**, *18*, 6679.
**DOI**: 10.1021/la0202374
50. Holt, K.; Bard, A.; *Biochemistry* 2005, *44*, 13214.
**DOI:** 10.1021/bi0508542
51. Amro, N.; Kotra, L.; Wadu-Mesthrige, K.; Bulchevy, A.; Mobashery, S.; Liu, G.; *Langmuir* **2000**, *16*, 2789.
**DOI:** 10.1021/la991013x
52. Barranco, S.; Spadaro, J.; Berger, T.; Becker, R.; *Clin. Orthop.* **1974**, *100*, 250.